



UNICO I+D Project
6G-SORUS-DRONE

SORUS-DRONE-A3.1-E1 (E12)

Initial Performance Evaluation

Abstract

In this deliverable, we conduct an in-depth analysis of strategies aimed at enhancing Beyond 5G (B5G) scenarios through the integration of Unmanned Aerial Vehicles (UAVs) and Reconfigurable Intelligent Surfaces (RIS). Our investigation focuses on critical Key Performance Indicators (KPIs) such as coverage probability, end-to-end delay, or power consumption. We systematically explore the dynamic interplay between these metrics under various influential factors shaping the B5G landscape, offering foundational insights into optimizing the deployment of UAVs and RIS.

Document properties

Document number	SORUS-DRONE-A3.1-E1
Document title	First Version of the Architecture
Document responsible	Pablo Serrano (UC3M)
Document editor	Pablo Serrano (UC3M)
Editorial team	Jonathan Almodóvar, Pablo Serrano (UC3M)
Target dissemination level	Public
Status of the document	Final
Version	1.0
Delivery date	31-12-2022
Actual delivery date	31-12-2022

Production properties

Reviewers	Marta Ferreira, Cristina Triviño (UC3M)
------------------	---

Disclaimer

This document has been produced in the context of the 6G-SORUS-DRONE Project. The research leading to these results has received funding from the Spanish Ministry of Economic Affairs and Digital Transformation and the European Union-NextGenerationEU through the UNICO 5G I+D programme.

All information in this document is provided "as is" and no guarantee or warranty is given that the information is fit for any particular purpose. The user thereof uses the information at its sole risk and liability.

Contents

List of Figures.....	4
1. Introduction	5
2. RIS Integration Strategies.....	7
3. Scenarios	8
3.1 UAV Mission Coverage.....	8
3.1.1. Single UAV	8
3.1.2. Multiple UAVs.....	9
3.2 Control Capacity Planning	10
3.3 Dynamic UAVs	11
4 Performance Evaluation.....	13
4.1 Coverage Probability.....	13
4.2 Power Consumption.....	14
4.3 Control Dynamics and Data Operations	15
4.4 RIS Gains.....	17
4.5 Cooperative UAVs.....	18
4.6 Dynamic UAVs.....	19
5 Summary and Conclusions.....	27
6. References.....	28

List of Figures

Figure 1. Single UAV mission for coverage area.....	9
Figure 2. Multiple uav coverage in a mission area.....	10
Figure 3. cOVERAGE PROBABILITY VS. POWER OF ANTENNAS UNDER DIFFERENT ALTITUDES.....	13
Figure 4. coverage probability vs. power of antennas with different gains	14
Figure 5. POWER CONSUMPTION VS. DISTANCE FOR DIFFERENT COVERAGE PROBABILITIES.....	15
Figure 6. percentile of sojourn time for different target delays in controller (left) and uav (right). ...	17
Figure 7. Coverage probability with multiple uavs in cooperation.....	19
Figure 8. gains of using ris vs. free space in terms of power consumption	18

1. Introduction

Recent advancements in aerial industry toward Unmanned Aerial Vehicles (UAVs) paved the way for a set of novel use cases in the sky, opening a new range of innovative applications. The varied sizes and shapes, coupled with the cost-effectiveness of UAVs, create opportunities in fields like package delivery, public safety, and medical support. UAVs can be broadly categorized into different types e.g., fixed-wing, rotary-wing, chopper drones, among others [SBM18].

The evolution of the aerial industry has seen a confluence with cutting-edge technologies like Reconfigurable Intelligent Surfaces (RIS), improving the capabilities of UAVs [LYL+22, YMZ+20, MMM+21]. RIS, with its ability to dynamically control and manipulate electromagnetic waves, plays a crucial role in enhancing communication and sensing capabilities of UAVs. By integrating RIS into the UAV systems, it becomes possible to optimize signal strength, mitigate interference, and adapt to dynamic environmental conditions, thereby significantly improving the overall performance and reliability of aerial operations. This synergy between UAVs and RIS not only extends the range of applications in fields such as surveillance and communication but also unlocks new possibilities in autonomous navigation and collaborative aerial missions [RTG+07].

This deliverable is organized as follows. Section 2 outlines the specific requirements guiding our analysis. These requirements encompass both technical specifications and contextual considerations, providing a clear framework for evaluating the effectiveness of UAVs and RIS in addressing the challenges posed by the evolving B5G landscape. Sections 3 and 4 delve into diverse scenarios and the subsequent performance evaluation, respectively. Section 3 is subdivided into three key subsections—UAV Radio, Control Capacity Planning, and Multiple UAVs—each delving into distinct aspects of the scenarios under consideration. These subsections lay the groundwork for our subsequent analysis by establishing the contextual framework. *UAV radio* delves into the intricate details of UAVs' radio communication aspects. By examining the UAV radio capabilities, we aim to identify strengths and limitations that play a pivotal role in shaping communication scenarios within B5G. *Control capacity planning* focuses on the packet-level dynamics, this subsection explores the efficiency of data transmission and reception in UAV networks. We investigate the packet-level intricacies to better understand the data flow and latency aspects crucial for B5G communication. *Multiple UAVs* envisions a multitude of interconnected devices, understanding the dynamics of multiple UAVs becomes imperative. This subsection explores the challenges and opportunities associated with the simultaneous operation of multiple UAVs, paving the way for robust communication strategies.

Section 4 evaluates the performance of UAVs and RIS in B5G scenarios. Subsections within this section explore critical KPIs, including Coverage Probability, Power Consumption, Control Dynamics and Data Operations, Cooperative UAVs, and RIS Gains. *Coverage Probability* delves into the coverage probability metrics, analyzing the extent to which UAVs and RIS contribute to ensuring reliable and expansive network coverage. Insights from this evaluation are essential for optimizing network

design to meet the demands of B5G scenarios. *Power Consumption* presents the power consumption patterns of UAVs and RIS, providing an understanding of their energy dynamics and paving the way for more energy-efficient solutions. *Control Dynamics and Data Operations* evaluates the reliability metrics, shedding light on the robustness and dependability of UAV and RIS-integrated networks. *Cooperative UAVs* investigates how cooperative efforts enhance overall system performance. This collaborative approach aligns with the collaborative nature of the envisioned B5G scenarios. *RIS Gains* focuses on the gains facilitated by Reconfigurable Intelligent Surfaces. By examining the impact of RIS on communication quality and efficiency, we aim to uncover the advantages these intelligent surfaces bring to the B5G landscape.

Through this deliverable, we highlight the intricate dynamics of UAV and RIS integration, providing a valuable resource for stakeholders navigating the evolving landscape of B5G communication networks.

2. RIS Integration Strategies

We outline the fundamental approaches that form the foundation for the analysis of UAV and RIS integration within Beyond 5G (B5G) scenarios. These requirements are carefully crafted to encompass both technical specifications and contextual considerations, ensuring a comprehensive evaluation of the performance metrics detailed in Section 4.

Coverage Probability Optimization. To ensure the effective deployment of UAVs and RIS within B5G scenarios, a fundamental requirement is the optimization of coverage probability (evaluated in Section 4.1). The integration must be designed to enhance the probability of reliable communication coverage across the targeted area. This involves strategically deploying UAVs and configuring RIS elements to maximize signal reach, minimizing coverage gaps, and thereby improving the overall reliability (as explored in Section 4.3) of the communication network.

Energy-Efficiency Standards. Sustainability is a guiding principle, necessitating adherence to energy-efficiency standards. The integration must optimize power consumption (as evaluated in Section 4.2) to align with energy-efficient solutions, ensuring the network's reliability and contributing to the overarching goal of environmentally sustainable B5G communication networks.

Cooperative Communication Protocols. Given the collaborative nature of UAVs (as explored in Section 4.4), the integration should incorporate cooperative communication protocols. This requirement aims to foster synergistic interactions among UAVs, enhancing not only coverage probability and reliability but also optimizing power consumption through collaborative efforts.

RIS Integration Strategies. Specific requirements are established for the seamless integration of Reconfigurable Intelligent Surfaces, addressing strategies for dynamically configuring RIS elements. This is essential not only for optimizing communication links, enhancing coverage probability and reliability but also for minimizing power consumption by strategically utilizing RIS capabilities (as explored in Section 4.4 and Section 4.2).

3. Scenarios

We consider a scenario with multiple UAVs and a single controller. UAVs are airborne vehicles equipped with wireless sensors and communication apparatus, enabling seamless connectivity to a network. This connectivity empowers them to relay information to a controller. The controller governs the entire UAV network. It bears the responsibility of overseeing and regulating network topology, resource allocation, global network visibility, traffic management, policy enforcement, failover and redundancy provision, and coordination with other controllers. Additionally, the controller undertakes the supervision of the UAV network, optimizing its performance, enforcing policies for UAV nodes. We specifically concentrate on two different scenarios: radio and packet. In the former, we delve into the intricacies of the radio component, exploring its capabilities. In the latter, we focus on studying performance at the packet level.

3.1 UAV Mission Coverage

In this scenario, we examine a situation in which UAVs must fulfil a specific coverage requirements for a designated area. Initially, we analyse a scenario involving a single UAV, and subsequently, we expand our investigation to encompass multiple UAVs.

3.1.1. Single UAV

We consider a single UAV operating within a designated mission cell, as illustrated in Figure 1[MSB+16]. In this UAV coverage scenario, the single UAV is assigned a crucial role in accomplishing a well-defined coverage objective. This scenario finds relevance across diverse applications such as surveillance, monitoring, search and rescue, and communication networks. The deployment of a single UAV within this context underscores its capability to effectively address coverage requirements within a specific area.

The single UAV's mission within the designated cell involves intricate navigation and surveillance tasks, optimizing its movements to ensure comprehensive coverage. This focused approach is particularly beneficial in scenarios where a targeted, precise inspection or data gathering is crucial.

Furthermore, the adaptability of a single UAV in this context enables cost-effective and resource-efficient solutions. The streamlined coordination and deployment of a single UAV contribute to operational simplicity, making it an ideal choice for scenarios where a more extensive fleet may not be necessary or feasible.

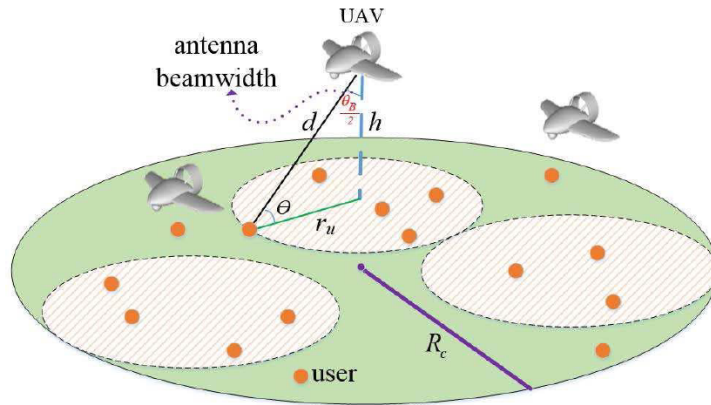


FIGURE 1. SINGLE UAV MISSION FOR COVERAGE AREA

As suggested by [MSB+16], we consider the following equation that models the coverage probability of a UAV:

$$P_{\text{cov}} = P_{\text{LoS},j} Q \left(\frac{P_{\min} + L_{dB} - P_t - G_{3\text{dB}} + \mu_{\text{LoS}}}{\sigma_{\text{LoS}}} \right) + P_{\text{NLoS},j} Q \left(\frac{P_{\min} + L_{dB} - P_t - G_{3\text{dB}} + \mu_{\text{NLoS}}}{\sigma_{\text{NLoS}}} \right),$$

where P_{LoS} and P_{NLoS} are the line of sight and non-line of sight links between the UAV and the ground users. These parameters depend on the elevation angle, environment, and relative location of the UAV and the users. P_{\min} is the minimum received power requirement (in dB) for a successful detection and P_t is the UAV's transmission power. L_{dB} is the path loss and $G_{3\text{dB}}$ is the UAV antenna gain. The mean and variance of the shadow fading for LoS and NLoS links are $(\mu_{\text{LoS}}, \sigma_{\text{LoS}}^2)$, and $(\mu_{\text{NLoS}}, \sigma_{\text{NLoS}}^2)$. The variance depends on the elevation angle and the environment

$$\sigma_{\text{LoS}}(\theta_j) = k_1 \exp(-k_2 \theta_j) \\ \sigma_{\text{NLoS}}(\theta_j) = g_1 \exp(-g_2 \theta_j)$$

where $\theta_j = \sin^{-1}(h/d_j)$ is the elevation angle between the UAV and the user, k_1 , k_2 , g_1 , and g_2 are constant values which depend on environment. Finally, $Q(\cdot)$ denotes the Q function.

3.1.2. Multiple UAVs

In this scenario, we delve into the complexities of a multiple UAV cooperative coverage scenario extending the equation of Section 3.1.1 for multiple UAVs [RWC+18]. In this dynamic setting, a synergy unfolds as multiple UAVs collaborate harmoniously to achieve a shared coverage objective. The inherent advantage of this cooperative approach lies in the collective effort of multiple UAVs, significantly enhancing the probability of coverage for the designated ground unit.

Within this collaborative framework, the increase in the number of UAVs directly correlates with an elevated likelihood of comprehensive coverage. This amplification effect is particularly advantageous in diverse applications, including surveillance, monitoring, search and rescue missions, and communication networks. The collaborative deployment of multiple UAVs adds a layer of efficiency and adaptability, allowing for more extensive coverage in a variety of operational scenarios.

We illustrate this cooperative scenario in Figure 2, where we present an example showcasing multiple UAVs working in cooperation to support a mission area. This visual representation encapsulates the coordinated efforts of the UAV fleet, demonstrating their ability to cover expansive areas efficiently and address complex operational requirements.

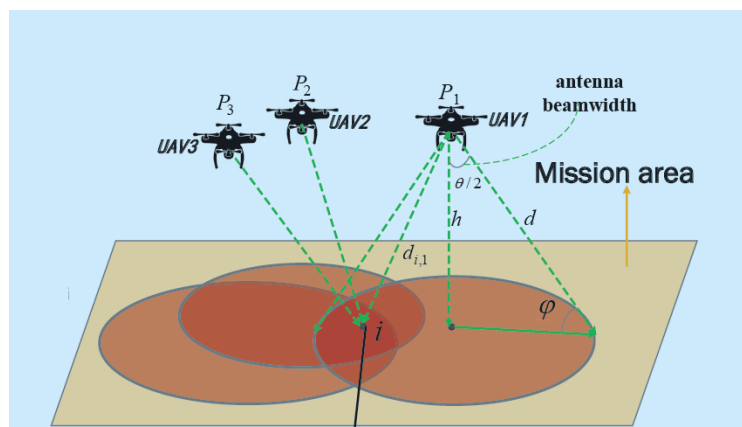


FIGURE 2. MULTIPLE UAV COVERAGE IN A MISSION AREA

3.2 Control Capacity Planning

Taking as reference the model in [ACJ23], we consider a scenario where the UAV is modeled as a M/M/1 queue and the controller as a M/M/c queue. The M/M/1 model offers simplicity in analysis and comprehension. It is applicable for modeling systems featuring a lone server and limitless buffer space. Furthermore, this model yields valuable insights into system performance and capacity. It adheres to a Poisson distribution, implying that packet service times follow an exponential distribution. The M/M/c model introduces the concept of c identical servers available for packet servicing. This approach proves efficient in situations where there is a high volume of traffic, necessitating multiple servers to process the packets. In this scenario, we have two different type of packets: data and control. Data packets are instrumental in transmitting mission-critical information, such as sensor data and images collected during the UAV's mission. These packets serve the primary function of conveying payload data to designated destinations. On the other hand, control packets play a pivotal role in managing and directing the UAV's activities and maintaining effective communication within the network. Responsible for transmitting commands and control signals, control packets ensure the coordinated execution of the UAV's mission, proper navigation, and network management. Together, the coexistence of data and control packets facilitates a well-

balanced and efficient operation of the UAV system, combining information transmission with effective system control.

We consider the following parameters of this scenario:

- Arrival rate of data packets
- Arrival rate of control packets
- Service time of data packets
- Service time of control packets
- Number of servers in the controller

3.3 Dynamic UAVs

In this scenario, we introduce a new dimension to the analysis, the dynamical behaviour of the UAVs. Understanding the aerodynamic forces and control mechanisms that govern UAVs allows for the design of more efficient flight paths, leading to reduced energy consumption and longer flight durations. The algorithms for understanding UAV's dynamics are detailed within Deliverable X. Here we present a model grounded on the concepts of Multi-Agent Systems (MAS) Orchestration. This model posits each UAV as an autonomous agent with a specific task to fulfil, including the use of potential field to optimize performance [CWH17, CSQ13].

In the framework, we explore how the orchestrated behaviour of Unmanned Aerial Vehicles (UAVs) in response to various critical elements, such as: other UAVs, Areas of interest (AOI) and areas of danger (AOD). All those elements are depicted in Figure 3. To understand and optimize UAV operations within this context, we must analyse the interactions across all elements:

UAV-to-UAV Interactions: This aspect focuses on how individual UAVs communicate and coordinate among themselves to achieve collective objectives. It encompasses formation flying and collision avoidance, ensuring efficient and harmonious operation within the UAV fleet.

UAVs and Areas of Interest: This dimension explores how UAVs interact with designated areas of interest (AOI). It involves UAVs approaching, and performing tasks within these zones, such as surveillance, data collection, or delivery activities.

UAVs and Avoidance Zones: Critical to UAV navigation is the ability to stay out of avoidance zones. These areas may represent restricted airspace, private buildings, or regions with high levels of interference. Understanding UAV responses to such zones is essential for ensuring safety, regulatory compliance, and operational integrity.

Avoidance Zones and Areas of Interest do not interact since they merely fill the space and serves as positional indicators for the UAVs.

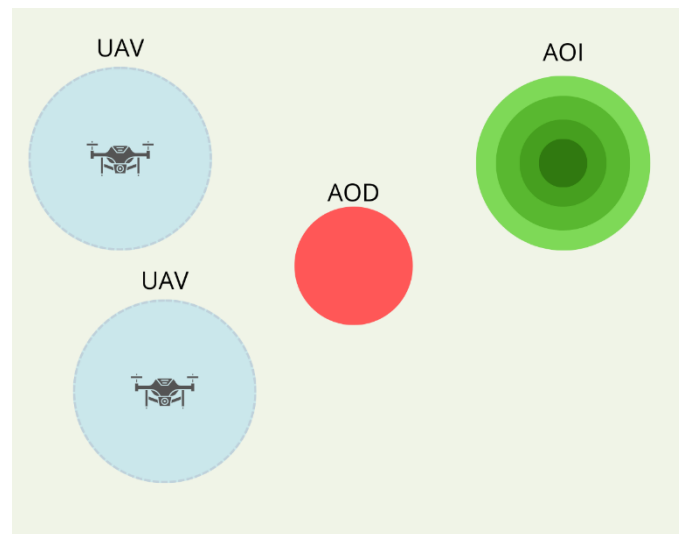


FIGURE 3. Different elements of the scenario. In grey is shown the UAVs with a coverage area in blue, in red is shown the area of danger (AOD) and in different shades of green is exposed the area of interest (AOI) which follows a distribution.

The parameters studied and analysed in this scenario are:

- Coverage radius of the UAVs. This parameter considers two things: the altitude of the UAV and the total area of coverage the UAV can guarantee.
- Speed of the UAVs. This parameter is also related with the durability and performance of the UAV.
- Distribution of AOI. The problem will drastically change when varying the distribution followed by the areas of interest.
- Distribution of AOD. Additionally, the number of danger zones affect the performance of the UAVs and might require longer flights and more coordinated behaviours.

4 Performance Evaluation

In this section we evaluate the system model under different conditions. First, we analyze the coverage probability in free space. We next evaluate the reliability as well and the power consumption of the antennas. Finally, we explore the benefits of incorporating Reconfigurable Intelligent Surfaces (RIS) specifically in terms of reliability.

4.1 Coverage Probability

The coverage probability indicates the probability that a given point or area on the ground is within the communication range of the UAV, meaning it can successfully establish and maintain a wireless link with that point. This metric is crucial for assessing the reliability and performance of communication systems in UAV applications, such as data transmission, remote sensing, or surveillance. We take as reference the scenario of Section 3.1.1. This scenario considers different parameters of the UAV such as UAV's carrier frequency, number of antenna elements, altitude between UAV and mission cell, elevation angle between UA and mission cell, UAV's carrier transmission power, environmental impact factor, among others.

In Figure 3, we examine the coverage probability across varying carrier transmission powers while adjusting the UAV's altitude relative to the ground. Our observation reveals that an increase in the carrier frequency power corresponds to an enhanced coverage probability, attributable to the stronger signal. Furthermore, as the UAV ascends, the coverage probability decreases, primarily due to path loss.

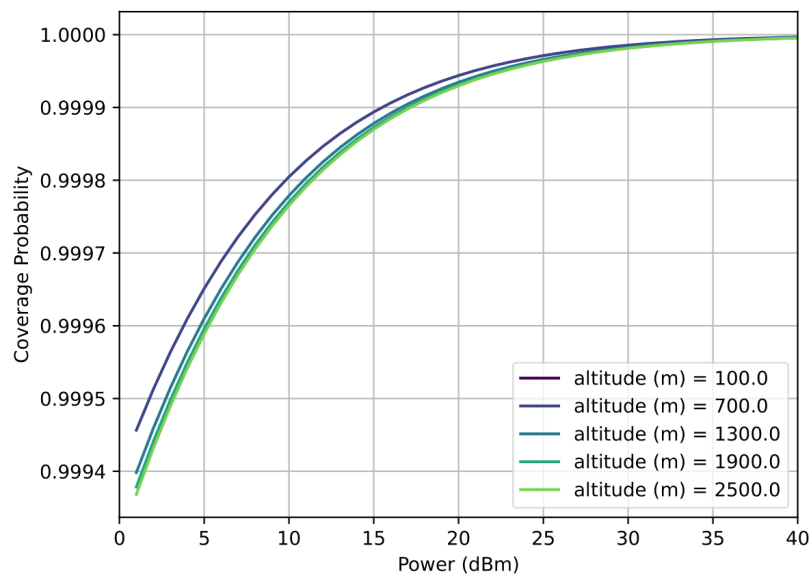


FIGURE 3. COVERAGE PROBABILITY VS. POWER OF ANTENNAS UNDER DIFFERENT ALTITUDES

In Figure 4, we delve into the coverage probability while adjusting the antenna gains under varying carrier transmission powers. We observe a direct correlation between increased carrier transmission

power and a higher coverage probability. Additionally, the heightened coverage probability with high antenna gains and increased carrier transmission power can be attributed to several key factors.

Firstly, higher carrier transmission power directly contributes to a more robust signal. The increased power of the transmitted signal enhances its reach and penetration, allowing for effective communication or sensing over longer distances. This boost in signal strength is a fundamental driver behind the observed improvement in coverage probability.

Moreover, the combined effect of high antenna gains and increased carrier transmission power results in a more potent and focused transmission. The antenna gains contribute to enhanced directivity, concentrating the signal in a specific direction, while higher transmission power ensures that this focused signal is more robust.

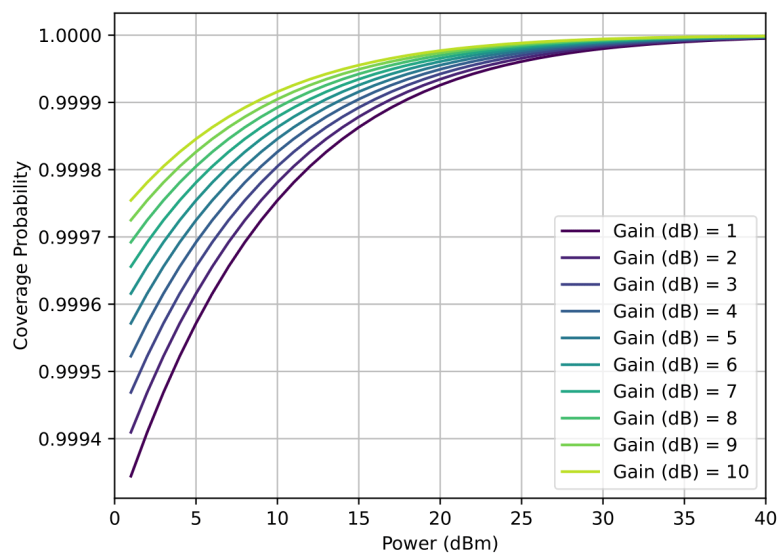


FIGURE 4. COVERAGE PROBABILITY VS. POWER OF ANTENNAS WITH DIFFERENT GAINS

4.2 Power Consumption

We next evaluate the power transmission to meet different target coverage probability requirements under different altitudes, i.e., distance between UAV and ground station (which is a centralized point on the floor for managing and monitoring the UAVs). Based in scenario of Section 3.1.1, we fix the target failure probability and compute the transmission power needed under different distances.

As the distance between the UAV and the ground increases, we observe in Figure 5 a corresponding increase in the power required by the UAV to maintain a certain coverage probability. This phenomenon can be attributed to free space path loss, a fundamental aspect of wireless communication. Free space path loss refers to the diminishing signal strength as a radiofrequency signal travels through unobstructed space.

As we observe an increase in the target coverage probability, we also note a corresponding rise in the power required by the UAV to meet these requirements. This phenomenon can be elucidated by

considering the trade-off between coverage and signal strength. A higher target coverage probability necessitates a more robust and widespread signal, especially in challenging environments with potential signal attenuation, interference, or obstacles. To achieve this heightened coverage probability, the UAV must compensate by increasing its transmitted power. The relationship between coverage probability and required power is intricately linked, reflecting the UAV's imperative to deliver a strong and reliable signal across a larger expanse to fulfil the specified coverage probability threshold. Thus, the observed escalation in power requirements is a strategic response to the increased stringency of the desired coverage probability.

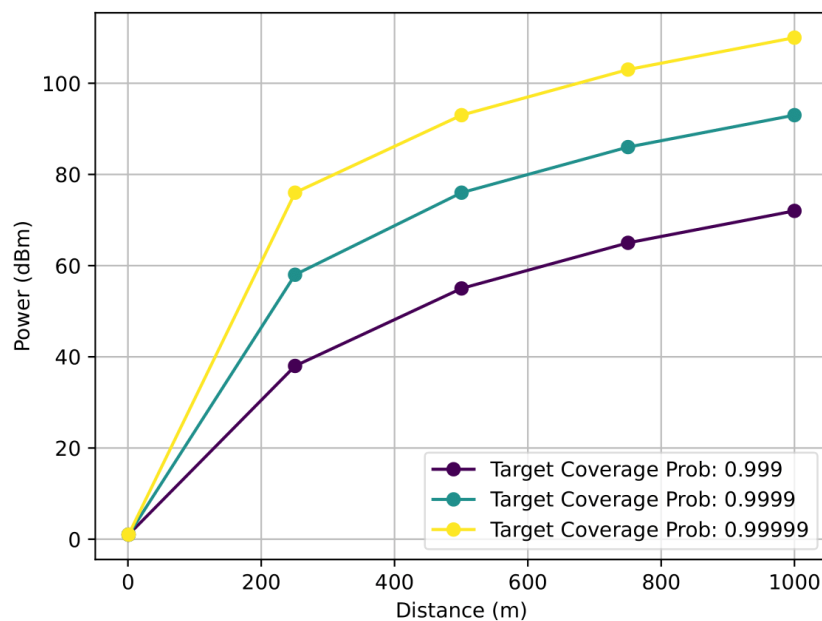


FIGURE 5. POWER CONSUMPTION VS. DISTANCE FOR DIFFERENT COVERAGE PROBABILITIES.

4.3 Control Dynamics and Data Operations

We conduct a packet-level evaluation to determine the percentile of the sojourn time, considering the scenario outlined in Section 3.2. The sojourn time percentile is an important measure. It indicates the point in the sojourn time distribution where a certain percentage of the data is below. For example, a 99th percentile of 40ms means that 99% of the packets take less than 40ms.

We consider both control and data packets. According to [HYM16], data rate demands are 24kpbs for telemetry and 5kpbs for control data exchange. This means that approximately 20% of the frame length is reserved for control purposes while the remaining 80% for data. Data traffic does not exhibit a deterministic or periodic pattern; instead, it tends to be bursty, leaning towards Poisson traffic.

Data packets. We consider real-time video stream following H.264/AVC flows. These flows contain I, B, P frames at rate λ_d , where the video frames are arranged in the so-called Group of Pictures (GOP). Following [KSG+05], we assume a GOP of size $N=12$ and that the frame length follows a

mixture of Gamma distributions. The weight assigned to each distribution is determined by the relative ratio of frames for each type (w_i), representing the proportion of frames of type i within the GOP. This ratio (w_i) is calculated as the number of frames of type i (n_i) divided by the total number of frames in the GOP (N), i.e.,

$$w_i = \frac{n_i}{N}$$

α_i and β_i are the shape and scale of the Gamma distribution. We assume the quantification with the highest quality in [KSG+05] (i.e., 10-10-10), which results in the numerical values for the parameters provided in the table below. It follows that the average video frame length is given by $l = w_I \alpha_I \beta_I + w_B \alpha_B \beta_B + w_P \alpha_P \beta_P = 260\text{kbits}$.

Type	w_i	α_i	β_i
I	1/12	16.487	21499
B	5/12	15.584	14608
P	6/12	17	15895

Following [RP06], the number of cycles to process a video frame is proportional to its length, with a constant of approx. 21.42 cycles/bit. Assuming a CPU operating at 150 MHz, the service time to process a video frame of length l_i is given by $s_i = l_i \times 21.42/250 [\mu\text{s}]$ and therefore the average service time per task is $s = 22.3 [\text{ms}]$.

Control packets. We consider control-related commands on the uplink (UL) channel. The uplink (UL) channel in UAVs is crucial for transmitting control-related commands from the ground control station or operator to the UAV. These commands are fundamental for orchestrating various aspects of the UAV's flight, navigation, and overall operation. They encompass a range of functionalities, including takeoff initiation, directing the UAV's landing procedure, and specifying waypoints that define the flight path [SK14]. Altitude and speed control commands ensure precision in flight dynamics, allowing adjustments to the UAV's height and speed as needed. In emergency situations, commands such as "Return to Home" (RTH) initiate an autonomous return to the launch location, while an

emergency stop command brings all UAV operations to an immediate halt. These packets follow a Poisson distribution with an inter-arrival rate between 10 and 20 ms, as suggested by [BKG+21].

We present the results in Fig. 6, showcasing the percentile of the sojourn time with the variation of the target delay from 10 to 100 ms. We assess the percentile of the sojourn time in both the controller (left) and UAV (right) across two packet types: data and control.

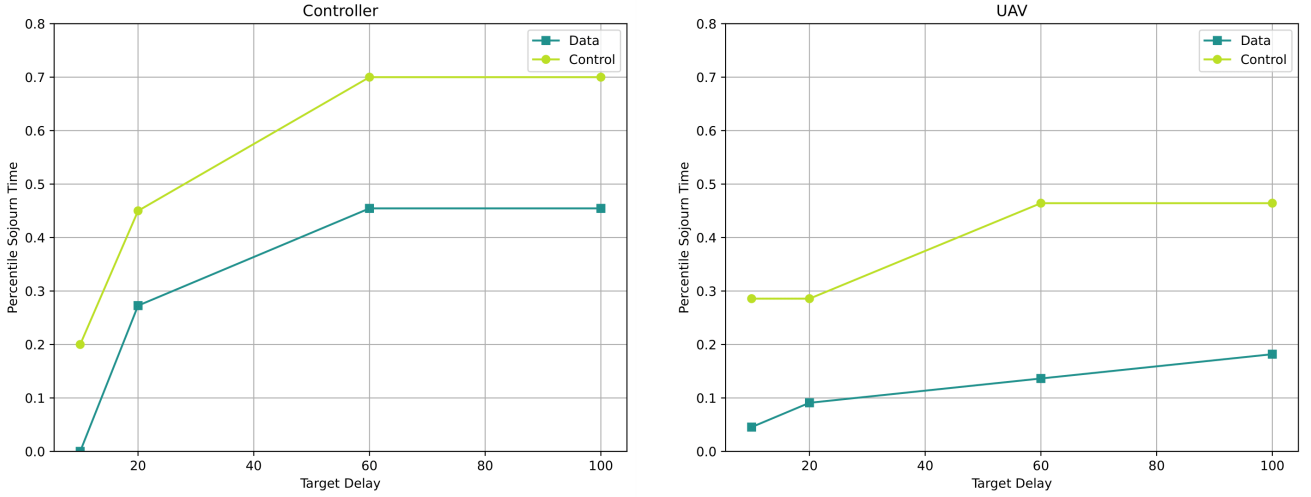


FIGURE 6. PERCENTILE OF SOJOURN TIME FOR DIFFERENT TARGET DELAYS IN CONTROLLER (LEFT) AND UAV (RIGHT).

In the controller, we observe that control packets exhibit a higher percentile than data packets, which is reasonable given that data packets are more numerous and larger in size than control packets. A similar trend is evident in the UAV, where control packets also demonstrate a higher percentile compared to data packets. It is noteworthy that, overall, the percentile in the controller for both data and control packets is notably higher than in the UAV, attributable to the superior computational power in the controller.

4.4 RIS Gains

We explore the advantages of using RIS in comparison with common antennas in the UAV, considering scenario 3.1.1. We take the path loss associated to RIS [E21] :

$$L_{RIS} = \left(\frac{\lambda}{4\pi}\right)^4 \left| \sum_{n=1}^N b_n \sqrt{\frac{G_e(-\hat{r}_n^i) G_e(\hat{r}_n^s)}{r_{i,n}^2 r_{s,n}^2}} e^{j\phi_n} \right|^2$$

Then, we calculate the power needed by the RIS to match different coverage probabilities under different distances between UAV and ground station. We present results in Figure 7.

We observe in Figure 7 a direct correlation between the increase in the distance between the UAV and the ground and a simultaneous rise in the power of the antennas. This relationship can be attributed to the phenomenon of free space path loss. As the UAV ascends and the distance from

the ground expands, the transmitted signals experience greater free space path loss, leading to a reduction in signal strength at the receiving end. To compensate for this signal attenuation and maintain effective communication or sensing, the UAV increases the power of its antennas. We also observe that as the target coverage probability increases, the power needed to satisfy the demands also increases. This phenomenon is intricately tied to the trade-off between coverage and signal strength. A higher target coverage probability necessitates a more robust and widespread signal to effectively cover the desired area.

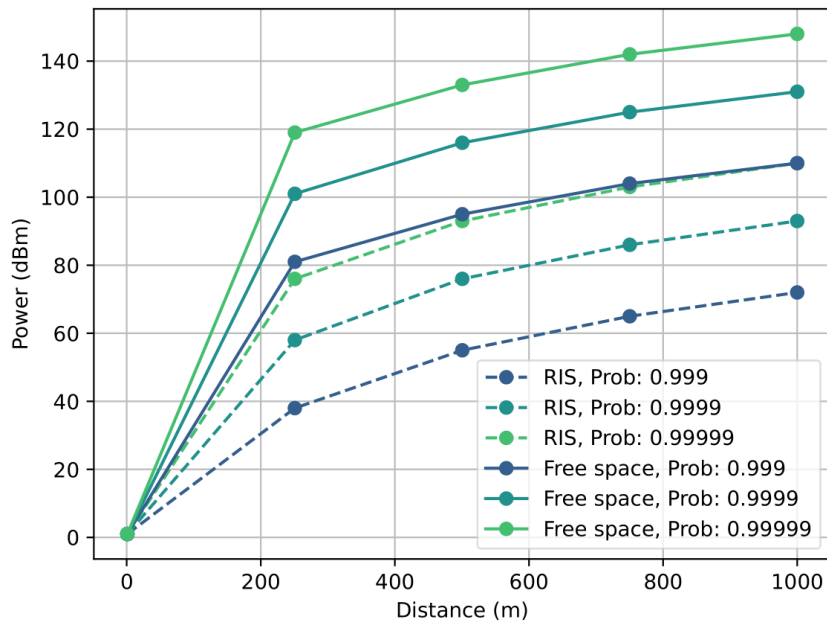


FIGURE 7. GAINS OF USING RIS VS. FREE SPACE IN TERMS OF POWER CONSUMPTION

Finally, we note that the incorporation of RIS elements results in a notable reduction of approximately 15% in the power required by the antenna. This reduction can be attributed to the unique capabilities of RIS in manipulating and optimizing the radiofrequency environment. RIS elements, when strategically deployed, can effectively mitigate signal losses and enhance signal strength.

4.5 Cooperative UAVs

We now explore how multiple UAVs can increase the coverage probability of a mission area. The cooperative interaction between multiple UAVs (as seen in Section 3.1.2) introduces a dynamic and adaptive dimension, enabling more comprehensive coverage, faster response times, and improved resilience to challenges. In the same fashion as in Section 4.1, we take as example five UAVs that provide a coverage probability of 76%. The results are depicted in Figure 8.

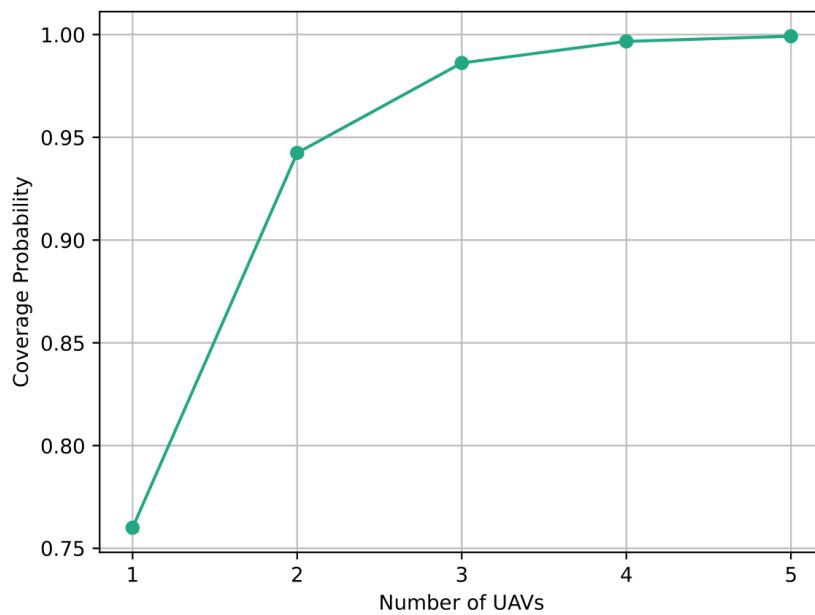


FIGURE 8. COVERAGE PROBABILITY WITH MULTIPLE UAVS IN COOPERATION

We find that as the number of UAVs increases the coverage probability is higher. This trend is a direct result of the collaborative synergy and collective capabilities inherent in a multi-UAV system. The increased number of UAVs enables more effective partitioning of the mission area, leading to a more thorough coverage across the entire designated space. With a larger fleet of UAVs, parallel monitoring and response capabilities are enhanced, enhancing the coverage outcomes.

4.6 Dynamic UAVs

Mathematically, this scenario can be defined as an optimization problem where we want to adjust the UAVs' positions such that they minimize the target function (move towards Areas of interest) while also avoiding collisions with each other and staying away from restricted areas. This problem is complex due to the competing objectives of attraction to the function's minimum and repulsion from other UAVs and the AOD.

This is just one possible implementation of the problem. Other approaches present a trade off between complexity and representativity. Alternative models consist of combining flocking and swarming effects to explore the coordination of UAVs [CLV15]; note that this implementation solely deals with the interactions among UAVs seeking for coordinated behaviour. Other models focus on the forces and momentums applied over the rotor blades that enable flying in a single UAV [FDZD13] [ref]. Our model may be simpler than this last one approach but the lack of complexity (computational) in the model allows for: analysis and deployment of several scenarios and more importantly, distributed computing of the algorithm; this is that each UAV is able to easily compute this algorithm in order complete tasks.

We will see that with the elements exposed in Figure 3 we can simulate complex scenarios that can be good representations of the reality.

The implementation involves iterating over a series of steps where each UAV's position is updated based on:

- The gradient of the target function, pushing the UAV towards the function's minimum.
- The cumulative repulsion forces from other UAVs, ensuring a safe distance is maintained between them.
- The repulsion force from the areas of danger, avoiding restricted areas.

Additionally, noise is introduced in the updates to simulate real-world uncertainties and prevent the UAVs from converging to a perfectly deterministic path. This noise can represent factors such as wind, measurement inaccuracies, or other unpredictable environmental conditions.

We will examine each of the interactions one by one:

- Gradient descent: This term represents the optimization of the positions of N UAVs, represented by coordinates (x_i, y_i) , this is done by updating their locations to approximate the minimum of the target function $f(x, y)$ which characterizes the Area of Interest (AOI). The efficacy and reliability of the gradient descent method hinge on the convexity of the target function. For convex functions, gradient descent provides a robust approach, assuring convergence towards the minimum.

$$(x_i, y_i) = (x_i, y_i) - \alpha \nabla f(x_i, y_i)$$

- Repulsion between UAVs: The interaction is modelled as a binary repulsion force mechanism between UAVs. Specifically, when the separation distance between any two UAVs diminishes below a critical threshold, defined as the sum of their radii, a repulsion force of magnitude \vec{F}_U is exerted in the opposite direction of their approach.

$$(x_i, y_i) = (x_i, y_i) - \vec{F}_U$$

- Repulsion between UAVs and AOD: The interaction is modelled again as a binary force. Specifically, when an UAV gets close enough to an AOD, the UAV feels a force in the opposite direction of magnitude \vec{F}_D .

$$(x_i, y_i) = (x_i, y_i) - \vec{F}_D$$

- Finally, we introduce an element of stochastic noise to the system. This addition serves a dual purpose, significantly enriching the realism and robustness of the simulation. This noise factor is meticulously parameterized by a variable β , allowing for precise control over its intensity and impact.

$$(x_i, y_i) = (x_i, y_i) + \beta(N(0,1), N(0,1))$$

Thus, the updated of the positions of the UAVs are given by:

$$(\mathbf{x}_i, \mathbf{y}_i)_{t+1} = (\mathbf{x}_i, \mathbf{y}_i)_t - \alpha \nabla f(\mathbf{x}_i, \mathbf{y}_i)_t - (\mathbf{0} | \overrightarrow{F_U}) + (\mathbf{0} | \overrightarrow{F_D}) + \beta(N(\mathbf{0}, \mathbf{1}), N(\mathbf{0}, \mathbf{1}))$$

Now, we carry out an exploration of how various parameters influence UAV behaviours through a series of targeted simulations. Each simulation is designed to incrementally increase in complexity, allowing us to isolate and understand the effects of specific variables within controlled environments.

Some parameters are fixed thought all simulations, these are:

- The learning rate of the gradient descent $\alpha = 0.1$
- The radius of coverage of the UAV $r_U = 0.4$
- The safe distance with respect to the AOD $r_D = 0.3$
- The forces that repel UAVs from UAVs and AOD $\overrightarrow{F_U} = \overrightarrow{F_D} = 0.05$
- The distribution of the POI is a gaussian distribution $N((2,2), (1,1))$

Single UAV with an AOI:

In Figure 9, we observe the trajectory followed by a single UAV as it navigates towards a designated Point of Interest (POI). It's important to note that the X and Y coordinates, are measured in Arbitrary Units (A.U.) of length. This choice of units allows for a generalized representation of the UAV's path, making the analysis broadly applicable across various scales and operational contexts.

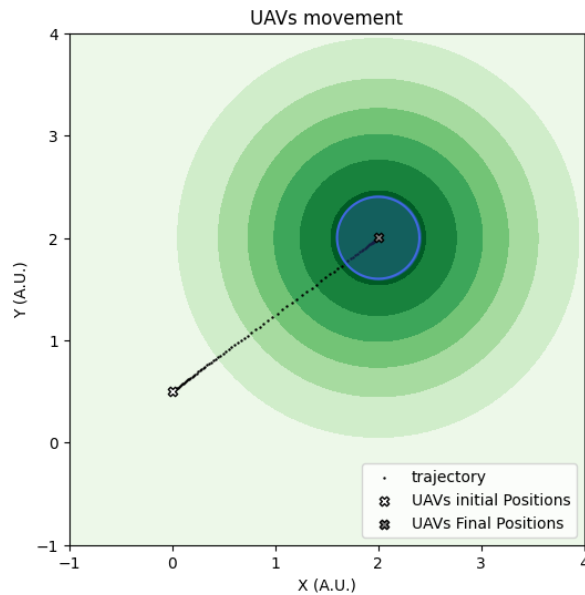


FIGURE 9. Trajectory of a single UAV moving towards an AOI.

Single UAV with an AOI and AOD:

Figure 10 illustrates the route of a UAV as it makes its way to the Area of Interest. The UAV's course leads to an encounter with an Area of Danger (AOD). Despite this incident, we can see the effectiveness of the UAV's navigational algorithm, which avoid such restricted zones.

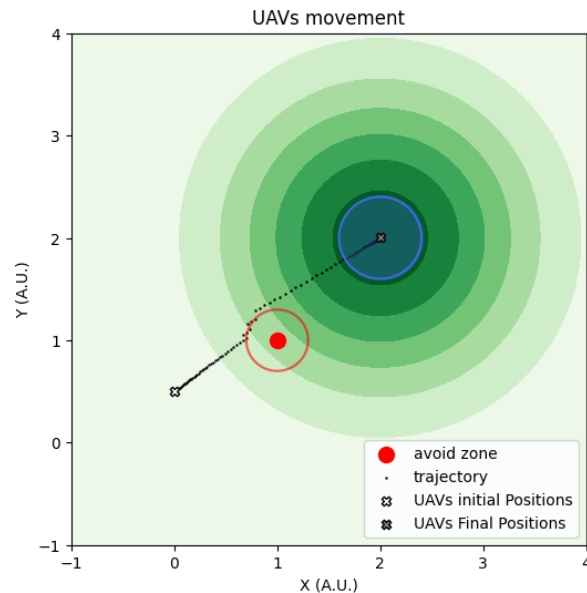


FIGURE 10. Trajectory of a single UAV moving towards an AOI colliding with an AOD.

Interaction between three UAVs:

Figure 11 depicts the dynamic trajectories of three Unmanned Aerial Vehicles (UAVs) as they navigate through space and interact with one another. As the UAVs converge along their flight paths, the repulsive forces come into play, causing them to diverge and maintain a safe distance from each other.

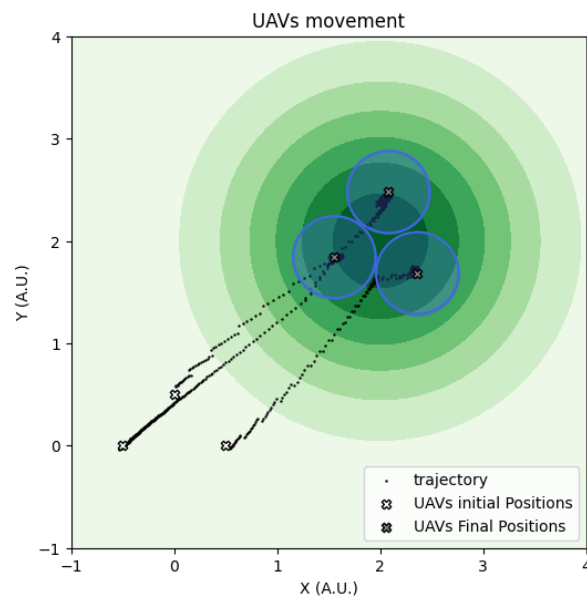


FIGURE 11. Trajectory of three UAVs moving towards an AOI colliding between them.

Interaction between three UAVs and an AOD:

Figure 12 shows three UAVs flying and avoiding an Area of Danger (AOD). At the end of the simulation, they get close to each other and repel away, but still avoid the AOD. In the end, they spread out in the same way as they did in an earlier scenario without the AOD. This shows their ability to dodge dangers and the robustness of the dynamics of the UAVs.

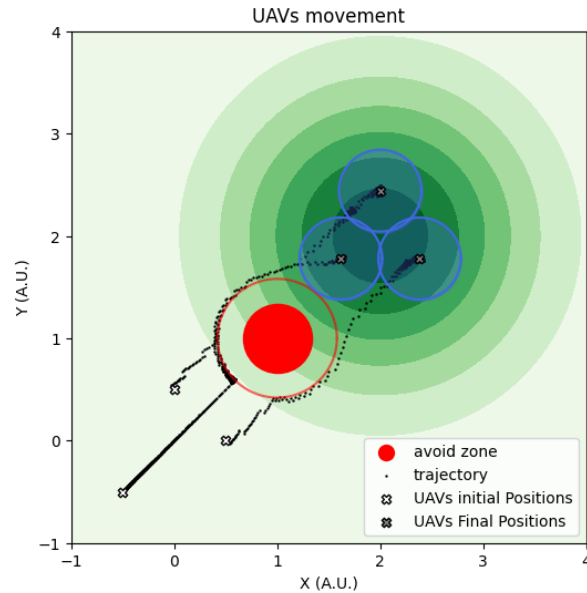


FIGURE 12. Trajectory of three UAVs moving towards an AOI colliding between them.

Stable distribution of the UAVs:

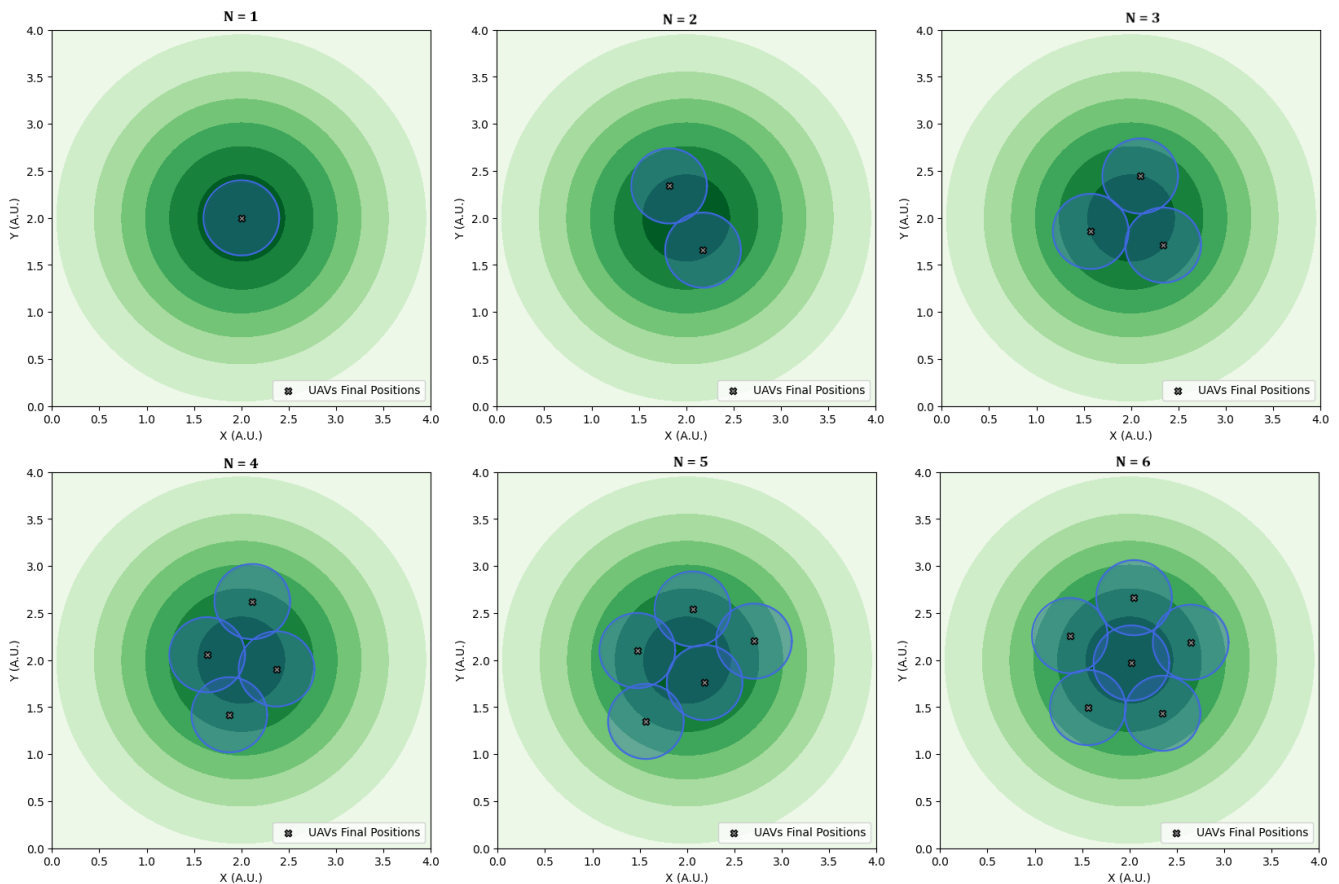


FIGURE 13. Stable distribution of the UAVs around the Area of Interest.

Figure 13 provides a visualization of the stable distribution of Unmanned Aerial Vehicles as a function of their quantity within a defined operational area. In essence, the Figure exposes the complex interplay between UAV quantity and effective area coverage. It argues for a strategic approach to UAV deployment, where the optimal number of UAVs is determined not merely by the size of the area to be covered but by the understanding of how UAVs interact with each other and with their environment to achieve stable and effective coverage.

Behaviour under complex scenario

Figure 14 explores the robustness of the algorithm performed by each UAV while trying to converge to one area of interest while avoiding several areas of danger. While the UAVs may enter for a moment these areas the UAVs are able to get out of them and still converge to a distribution like the ones seen before.

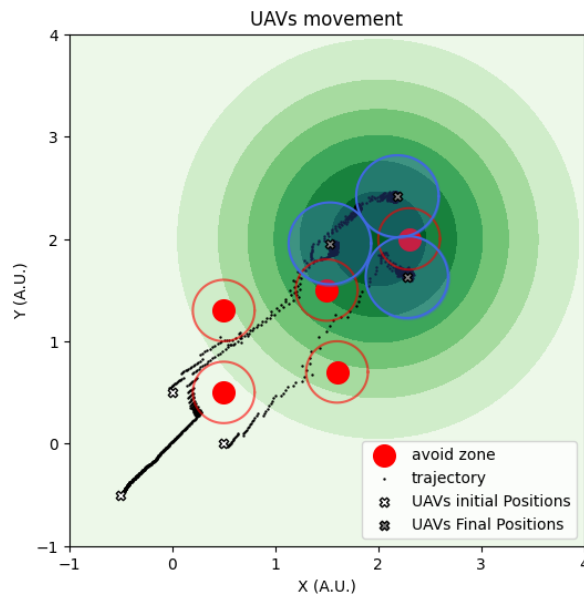


FIGURE 14. Trajectory of three UAVs in a scenario with different AOD.

Number of POI vs Number of UAVs

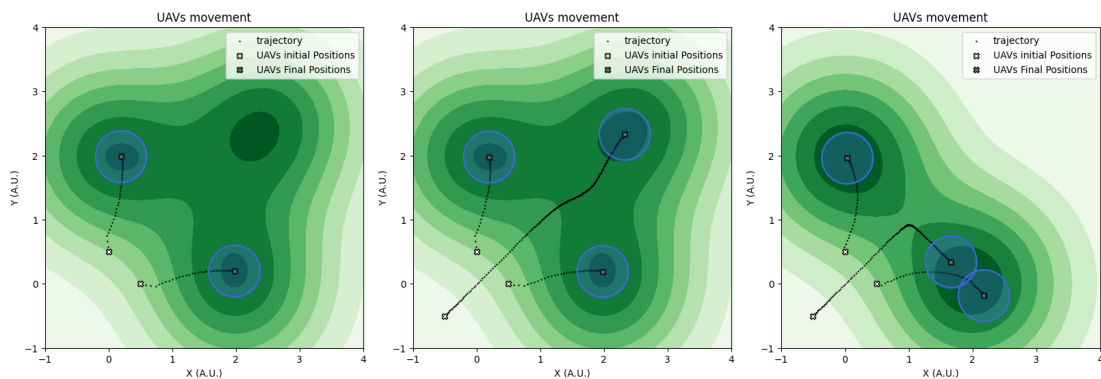


FIGURE 14. Trajectory of three UAVs in a scenario with different AOD.

Figure 14 explores the dynamics of UAV operations as the number of Areas of Interest (AOIs) varies, exposing the strategic importance of optimal configuration in diverse scenarios. Specifically, the illustration on the left highlights a critical insight: the adequacy of UAV numbers in relation to AOIs significantly influences mission success. For instance, with three designated AOIs and only two UAVs in play, it becomes impossible to achieve comprehensive coverage of all areas of interest. This demonstrates the necessity of aligning the number of UAVs with the mission objectives to ensure effective area coverage.

Conversely, In the image on the right we explore how the stable distribution of UAVs is affected by their initial positioning, a factor crucial for the successful application of gradient descent methods, especially in environments characterized by multiple potential minima. Addressing this complexity involves strategic parameter adjustments to ensure reliable convergence towards the intended targets. For example, enhancing the repulsion force among UAVs could encourage a more dispersed search pattern, enabling each UAV to independently target distinct minima. Furthermore, explicitly

assigning a specific AOI to each UAV ensures that every UAV is focused on converging towards its designated target area.

5 Summary and Conclusions

In this deliverable, we focus on an in-depth analysis of various methodologies aimed at enhancing the performance of Beyond 5G (B5G) scenarios. These scenarios aim at enhancing the capabilities of UAV-networks through the strategic integration of Unmanned Aerial Vehicles (UAVs) and Reconfigurable Intelligent Surfaces (RIS). To evaluate the performance, we delve into fundamental metrics such as coverage probability, area of coverage, sojourn time of delay suffered by packets, power consumption, meticulously examining their dynamics under the influence of key factors that shape the B5G landscape. Through analysis and experimentation, we aim to unravel insights into the intricate interplay between UAVs, RIS, and the dynamic elements that impact network performance.

6. References

- [ACJ23] M. A. B. S. Abir, M. Z. Chowdhury and Y. M. Jang, "A Software-Defined UAV Network Using Queueing Model," in *IEEE Access*, vol. 11, pp. 91423-91440, 2023, doi: 10.1109/ACCESS.2023.3281421.
- [BKG+21] A. Baltaci *et al.*, "Experimental UAV Data Traffic Modeling and Network Performance Analysis," *IEEE INFOCOM 2021 - IEEE Conference on Computer Communications*, Vancouver, BC, Canada, 2021, pp. 1-10, doi: 10.1109/INFOCOM42981.2021.9488878.
- [CLV15] M. G. C. A. Cimino, A. Lazzeri and G. Vaglini, "Combining stigmergic and flocking behaviors to coordinate swarms of drones performing target search," *2015 6th International Conference on Information, Intelligence, Systems and Applications (IISA)*, Corfu, Greece, 2015, pp. 1-6, doi: 10.1109/IISA.2015.7387990.
- [E21] Ellingson, S. W. (2021, September). Path loss in reconfigurable intelligent surface-enabled channels. In *2021 IEEE 32nd Annual International Symposium on Personal, Indoor and Mobile Radio Communications (PIMRC)* (pp. 829-835). IEEE.
- [FDZD13] H. C. T. E. Fernando, A. T. A. De Silva, M. D. C. De Zoysa, K. A. D. C. Dilshan and S. R. Munasinghe, "Modelling, simulation and implementation of a quadrotor UAV," *2013 IEEE 8th International Conference on Industrial and Information Systems*, Peradeniya, Sri Lanka, 2013, pp. 207-212, doi: 10.1109/ICIIInfS.2013.6731982.
- [HYM16] Hayat, S., Yanmaz, E., & Muzaffar, R. (2016). Survey on unmanned aerial vehicle networks for civil applications: A communications viewpoint. *IEEE Communications Surveys & Tutorials*, 18(4), 2624-2661.
- [KSG+05] Koumaras, H., Skianis, C., Gardikis, G., & Kourtis, A. (2005). Analysis of H. 264 video encoded traffic. In Proceedings of the 5th International Network Conference (INC2005) (pp. 441-448).
- [LYL+22] Liu, X., Yu, Y., Li, F., & Durrani, T. S. (2022). Throughput maximization for RIS-UAV relaying communications. *IEEE Transactions on Intelligent Transportation Systems*, 23(10), 19569-19574.
- [MMM+21] Michailidis, E. T., Miridakis, N. I., Michalas, A., Skondras, E., & Vergados, D. J. (2021). Energy optimization in dual-RIS UAV-aided MEC-enabled internet of vehicles. *Sensors*, 21(13), 4392.
- [MSB+16] M. Mozaffari, W. Saad, M. Bennis and M. Debbah, "Efficient Deployment of Multiple Unmanned Aerial Vehicles for Optimal Wireless Coverage," in *IEEE Communications Letters*, vol. 20, no. 8, pp. 1647-1650, Aug. 2016, doi: 10.1109/LCOMM.2016.2578312.
- [RTG+07] Ryan, A., Tisdale, J., Godwin, M., Coatta, D., Nguyen, D., Spry, S., ... & Hedrick, J. K. (2007, July). Decentralized control of unmanned aerial vehicle collaborative sensing missions. In *2007 American Control Conference* (pp. 4672-4677). IEEE.

- [RP06] M. Roitzsch and M. Pohlack, "Principles for the Prediction of Video Decoding Times Applied to MPEG-1/2 and MPEG-4 Part 2 Video," 2006 27th IEEE International Real-Time Systems Symposium (RTSS'06), Rio de Janeiro, Brazil, 2006, pp. 271-280, doi: 10.1109/RTSS.2006.36.
- [RWC+18] L. Ruan *et al.*, "Energy-efficient multi-UAV coverage deployment in UAV networks: A game-theoretic framework," in *China Communications*, vol. 15, no. 10, pp. 194-209, Oct. 2018, doi: 10.1109/CC.2018.8485481.
- [SBM18] Singhal, G., Bansod, B., & Mathew, L. (2018). Unmanned aerial vehicle classification, applications and challenges: A review.
- [SK14] Suicmez, E. C., & Kutay, A. T. (2014, May). Optimal path tracking control of a quadrotor UAV. In 2014 International Conference on Unmanned Aircraft Systems (ICUAS) (pp. 115-125). IEEE.
- [YMZ+20] Yang, L., Meng, F., Zhang, J., Hasna, M. O., & Di Renzo, M. (2020). On the performance of RIS-assisted dual-hop UAV communication systems. *IEEE Transactions on Vehicular Technology*, 69(9), 10385-10390.